INORGANIC MATERIALS AND NANOMATERIALS

Composite solid electrolytes MWO_4–SiO_2 (M = Ca, Sr) and $Ln_2W_3O_{12}$–SiO_2 (Ln = La, Nd): synthesis and study of electrical transport properties

A. Guseva[a], N. Pestereva[a, *]

[a]*Ural Federal University , Yekaterinburg, 620002 Russia*

**e-mail: Natalie.Pestereva@urfu.ru*

Received by the editors on July 04, 2024.

Revised September 18, 2024

Accepted for publication October 04, 2024

Composite solid electrolytes based on alkaline earth tungstates MWO_4–SiO_2 (M = Ca, Sr) and rare earth metals $Ln_2W_3O_{12}$–SiO_2 (Ln = La, Nd)with the addition of nanodispersed silicon oxide were synthesized and their morphology, thermal, structural and electrical transport properties were studied. The absence of thermal effects on DSC of tungstates and silica mixtures as well as the absence of reflections of any foreign phases in the diffraction patterns of the composites, confirms their thermodynamic stability. The ionic nature of the composite conductivity is confirmed by the high values of ionic transfer numbers about 0.8 – 0.9 (EMF method) and the horizontal plot of conductivity versus oxygen pressure in the gas phase. The concentration dependence of the conductivity of the composites $(1–x)MeWO_4–xSiO_2$ (M = Ca, Sr), $(1–x)Ln_2W_3O_{12}–xSiO_2$ (Ln = La, Nd) passes through a maximum at x = 0.03–0.30 (x – mole fraction). The $0.70Nd_2W_3O_{12}–0.30SiO_2$ composite has the best conductivity of $3.2\cdot10^{-2}$ S/cm at 900°C.

Keywords: heterogeneous doping, tungstates of alkaline earth and rare earth metals, nanodisperse silicon oxide

DOI: 10.31857/S0044457X250114e6

INTRODUCTION

Nanodispersed silicon oxide (along with aluminum oxide) is traditionally used as a heterogeneous additive to ion conductors in order to obtain composite solid electrolytes [1-6]. The composite conduction effect, i.e., a sharp increase in the conductivity of ionic conductors during their heterogeneous doping with inert highly dispersed additives, is due to boundary effects, therefore, the area of the solid

electrolyte/dispersed additive interface plays a key role in its implementation. SiO2 occupies a special place among the variety of dispersoids added to solid electrolytes. This is due to its accessibility, chemical inertia, and comparative ease of production in a highly dispersed state. The properties of composites based on alkali-earth metal salts [1-6] with cationic conductivity have been most well studied.

SCHZM tungstates MWO4 (M = Ca, Sr, Ba) with the structure of scheelite and rare earth metals (REM) Ln2W3O12 (Ln = La, Sm, Eu, Gd, Nd) with the structure of defective scheelite, solid solutions and composites based on them are widely used in engineering as components of laser materials and catalysts [7-14]. Recent studies of their electric transport properties have shown that these substances may also be of interest as materials for ionics. It was established in [15, 16] that oxygen ions are the main charge carriers in these substances. However, the ionic conductivity of SCHZM and REM tungstates is not high enough (10-5-10-4 Cm/cm at 900 °C) for practical use. Since the addition of highly dispersed SiO2 to ionic salts, according to [1-6], leads to an increase in conductivity by up to two orders of magnitude, in this work an attempt was made to improve the oxygen conductivity of SCHZM and REM tungstates by heterogeneous doping with nanodispersed silicon oxide.

EXPERIMENTAL PART

Tungstates of alkaline earth metals MWO_4 (M = Ca, Sr) and rare earth metals $Ln_2W_3O_{12}$ (Ln = La, Nd) were synthesized by solid-phase method from MCO_3 (or Ln_2O_3) and WO_3 of "extra pure" grade. Calcium and strontium carbonates were preliminarily annealed at 400°C, lanthanum and neodymium oxides at 1200°C, and tungsten oxide at 500°C for 4 hours to remove adsorbed moisture and hydroxyl groups from the surface of crystallites. The synthesis was carried out in air according to the equations:

$$MCO_3 + WO_3 \rightarrow MWO_4 + CO_2; \quad (1)$$

$$Ln_2O_3 + 3WO_3 \rightarrow Ln_2W_3O_{12}. \quad (2)$$

The mixture of reagents, taken in stoichiometric amounts, was heated in air with a gradual temperature increase from 700 to 1000 - 1050°C in four stages with intermediate grinding in ethanol. The synthesis mode of tungstates is shown in Table 1.

Composites (1- x)MWO_4 - x SiO_2 and (1- x)$Ln_2W_3O_{12}$ - x SiO_2, where x is the molar fraction of SiO_2, were prepared by mechanical mixing of powders of the corresponding metal tungstate and highly dispersed silicon dioxide of high purity with SiO_2 content of 99.9% (trade name Aerosil-300, Degussa) with a specific surface area of 300 m^2/g (average particle size 7 nm).

The relationships between molar and volume fractions of SiO_2 are presented in Table 2.

Thoroughly ground mixtures of corresponding tungstate powders and SiO_2 in ethanol medium were pressed on a manual hydraulic press into disk-shaped briquettes with a diameter of 10 mm and a thickness of 2 mm under a pressure of 50 MPa. The pressed briquettes were slowly heated in a furnace to 950°C (for $La_2W_3O_{12}$–SiO_2) or 1000°C (for MWO_4–SiO_2 (M = Ca, Sr) and $Nd_2W_3O_{12}$–SiO_2) and annealed for 24 h.

The experimental density of the composite briquettes was determined by their dimensions and mass:

$$\rho_{эксп} = \frac{m}{V}, \qquad (3)$$

where ρ_{exp} is the experimental density of the briquette, m is the mass of the briquette, V is the volume of the briquette.

The theoretical density values of the composites were calculated using the formula:

$$\rho_{теор.\ комп} = \left(\rho_{теор\,(SiO2)} \cdot \varphi\right), \qquad (4)$$

where ρ_{theor} is the theoretical density value of the metal tungstate substance, φ is the volume fraction of SiO_2 in the composite, $\rho_{theor}(CaWO_4) = 6.09\ g/cm^3$, $\rho_{theor}(SrWO_4) = 6.2\ g/cm^3$, $\rho_{theor}(La_2W_3O_{12}) = 6.63\ g/cm^3$, $\rho_{theor}(Nd_2W_3O_{12}) = 7.04\ g/cm^3$, $\rho_{theor}(SiO_2) = 2.65\ g/cm^3$ [17, 18].

The effective density of briquettes was calculated using the formula:

$$\rho_{эф} = \frac{\rho_{эксп}}{\rho_{теор}} \times 100\% . \quad (5)$$

No correlation was found between the effective density of the composite and its composition. For all four studied systems, the effective density of the composite varied within 10% with different SiO_2 content. As an example, Fig. 1 shows the effective density of $(1-x)Nd_2W_3O_{12} - x\,SiO_2$ composites with different content of dispersed additive.

Table 3 shows the average values of effective density for the four studied systems.

For electrical measurements, porous Pt electrodes were applied to the end surfaces of the briquettes and sintered at 1000°C for 1 h.

X-ray diffraction analysis (**XRD**) of calcium, strontium, lanthanum, neodymium tungstates and composites based on them was carried out using a Bruker D8 Advance diffractometer with Cu K_α-radiation.

The morphology of composites and their elemental composition were studied by electron microscopy and energy dispersive analysis (**SEM-EDS**) of fractured sample briquettes using an Evo LS-10 Carl Zeiss NTS scanning electron microscope (CKP IENiM UrFU). Images of the surface of the studied materials were obtained using backscattered electron (BSE mode) and secondary electron (SE mode) detectors.

Simultaneous thermal analysis TG and DSC was performed on a Netzsch STA 409 PC Luxx instrument with a QMS 403 Aëolos quadrupole mass spectrometer. An equimolar mixture of powders of the corresponding tungstate and SiO_2 was heated from 50 to 1000°C at a rate of 10 degrees/min, the heating time was 95 min.

The electrical conductivity of calcium, strontium, lanthanum, neodymium tungstates and composites $(1-x)MWO_4 - x\,SiO_2$ and $(1-x)Ln_2W_3O_{12} - x\,SiO_2$ was measured by impedance spectroscopy using an Immittance Parameters Meter IPI1 (Trapeznikov Institute of Control Sciences, Moscow) in the frequency range of 500 Hz-200 kHz (the amplitude of the test signal automatically changes in the range of 3-300 mV) in the temperature range of 500-900°C. The temperature dependence of electrical

conductivity was measured in cooling mode at a rate of 1 degree/min. The dependence of conductivity on oxygen partial pressure was measured under isothermal conditions. The oxygen pressure was set using a ZirconiaM device and controlled by an oxygen pump and a solid electrolyte sensor based on $ZrO_2(Y_2O_3)$.

The method of EMF was used to determine the sum of ionic transport numbers of composites, based on the use of concentration galvanic cells. To create a gradient of oxygen partial pressure, one of the electrodes was forcibly purged with oxygen ($P_{O_2}^{//}$ = 1 atm), the other with air ($P_{O_2}^{/}$ = 0.21 atm) using a microcompressor. Isolation of the electrode gas spaces was achieved by careful grinding of the briquettes and pressing them against an alundum tube. The sum of ionic transport numbers was calculated using the Nernst formula for conductors with mixed conductivity:

$$E = \frac{RT}{4F} \cdot \Sigma t_{\text{ион}} \cdot ln\frac{P_{O_2}^{//}}{P_{O_2}^{/}}, \qquad (6)$$

where R is the molar gas constant, T is the temperature in K, F is the Faraday constant, Σt_{ion} is the sum of ionic transport numbers, $P_{O_2}^{//}$ is the partial pressure of oxygen equal to 1 atm, $P_{O_2}^{/}$ is the partial pressure of oxygen equal to 0.21 atm.

RESULTS AND DISCUSSION

X-ray phase analysis results

According to XRD data, calcium, strontium, lanthanum, and neodymium tungstates were obtained as single-phase materials, while the composites $(1-x)MWO_4 - x\,SiO_2$ and $(1-x)Ln_2W_3O_{12} - x\,SiO_2$ contained two phases: the desired tungstate and SiO_2 (Fig. 2). Thus, there is no chemical interaction between the substances that make up the composite.

X-ray diffraction pattern of SiO_2 is represented by a diffuse maximum at 2θ = 22.0°, which is characteristic for amorphous SiO_2 (ICDD No. 29-0085), as well as quartz reflections: 2θ = 28.7°, 33.3° (ICDD No. 83-540). The X-ray diffraction patterns

of composites $0.5Nd_2W_3O_{12}–0.5SiO_2$, and $0.7La_2W_3O_{12}–0.3SiO_2$ show all the reflections of tungstates, as well as a diffuse peak of amorphous SiO_2 at 22°, while the other reflections of SiO_2 (2θ = 28.7°, 33.3°) coincide with the reflections of tungstates (shown by arrows in Fig. 2). Since nanodispersed SiO_2 is highly amorphized, the X-ray diffraction patterns of composites $(1– x)MWO_4 – x SiO_2$ (M = Ca, Sr) do not show silicon oxide reflections against the background of crystalline calcium and strontium tungstate reflections (Fig. 2). No reflections of foreign phases were found in the X-ray diffraction pattern of the composites, indicating the absence of interaction between the composite components.

Results of thermogravimetric analysis and differential scanning calorimetry

The results of TG-DSC of equimolar mixtures of tungstates and SiO_2 are presented in Fig. 3. It can be seen that in the temperature range from 20 to 1000°C, the mass of the mixture of tungstates and silicon oxide practically does not change, and thermal effects are absent. These data indicate the thermodynamic stability of the composites up to 1000°C: the components of the composite (tungstate and silica) do not react with each other. For all the systems studied, the mass remains unchanged during heating; the figure shows data for the $0.5CaWO_4–0.5SiO_2$ system, however, such behavior is characteristic of all samples.

Results of electron microscopy and energy dispersive analysis

The morphology of the composites and their elemental composition were studied by SEM-EDS. Electron micrographs of fractures of composite briquettes of various compositions and EDS results are presented in Fig. 4.

The grain size of alkaline earth metal and rare earth metal tungstates varies from 2 to 20 μm. The EDS spectrum of large grain surfaces shows the presence of W and metal (Ca, Sr, La, or Nd), as well as a small amount of silicon. This allows identification of large grains as alkaline earth metal or rare earth metal tungstates. The exact size of silica grains could not be determined due to insufficient resolution, but it is significantly

less than 1 μm. The EDS spectrum in areas of small grain accumulation shows predominant silicon content with small amounts of tungsten and alkaline earth or rare earth metals.

For all systems, "retraction" of small SiO_2 grains into the near-surface layers of large tungstate grains was observed. This effect, previously discovered by us for tungstate composites with highly dispersed alumina additives [19], is explained by the lower surface energy of tungstates compared to the surface energy of refractory SiO_2 or Al_2O_3. For the composite $0.7Nd_2W_3O_{12}–0.3SiO_2$ (Fig. 4d), "immersion" of small silica grains into large neodymium tungstate grains is visible, especially at their junctions. In some cases, as for example in the composite $0.75SrWO_4–0.25SiO_2$ (Fig. 4b), the surface of tungstate grains where the cleavage occurred appeared "pitted" due to mechanical removal of SiO_2 grains during briquette cleavage. The EDS spectrum of this area shows a high silicon content compared to strontium and tungsten: [Si]/[Sr] ~ 20.

Investigation of electrotransport properties of composites

The conductivity polytherms of pure tungstates and composites with the same silica content ($0.7MWO_4–0.3SiO_2$ and $0.7Ln_2W_3O_{12}–0.3SiO_2$ respectively) in Arrhenius coordinates are presented in Fig. 5.

No clear correlation was found between the conductivity of composites and the type of crystal lattice or the conductivity value of metal tungstates that make up the composite. Lanthanum and neodymium tungstates are isostructural and have a defective scheelite lattice [20, 21]; however, the composite based on $Nd_2W_3O_{12}$ has the highest conductivity among those studied, while the composite based on $La_2W_3O_{12}$ has the lowest: the electrical conductivity of $0.7Nd_2W_3O_{12}–0.3SiO_2$ is 2.5 orders of magnitude higher than the electrical conductivity of $0.7La_2W_3O_{12}–0.3SiO_2$. Meanwhile, the difference in electrical conductivity between lanthanum and neodymium tungstates is not so large and is only 0.5 orders of magnitude [15, 22].

The conductivity of composites based on alkaline earth metal tungstates has an intermediate value in the studied series. Calcium and strontium tungstates are isostructural and have a scheelite crystal lattice [23]. For composites based on them, there is a correlation with the matrix conductivity: the electrical conductivity of $0.7CaWO_4–0.3SiO_2$ is about 0.5 orders of magnitude higher than the electrical conductivity of $0.7SrWO_4–0.3SiO_2$, the same ratio of electrical conductivity values is observed for the corresponding tungstates [24]. The effective activation energy of the composites' conductivity is 0.9–1.3 (± 0.1) eV in the entire studied temperature range.

To confirm the ionic nature of the composites' conductivity, its pressure dependence was investigated (Fig. 6). The electrical conductivity of the studied composites is practically independent of P_{O_2}, which indicates its ionic nature.

The same result is provided by measurements of the sum of ionic transport numbers of the composites using the EMF method (Fig. 7). The values of the sum of ionic transport numbers are in the range of 0.8–0.9, i.e., ionic transport dominates in the composites.

Fig. 8, shows the concentration dependences of the conductivity of the composites $(1-x)MWO_4-x\,SiO_2$ and $(1-x)Ln_2W_3O_{12}-x\,SiO_2$. For ease of comparison, the relative electrical conductivity of the composites σ/σ_o is shown, i.e., the ratio of the composite conductivity to the conductivity of the metal tungstate.

Since it is reliably established that electrical transfer in composites occurs along the matrix-dispersed additive interfacial boundaries [25-27], the maximum value of electrical conductivity is achieved for composites with the highest area of interfacial boundaries $MWO_4|SiO_2$ or $Ln_2W_3O_{12}|SiO_2$. For the studied composites, the maximum on the concentration dependence of conductivity corresponds to the silica content in the composite from 3 mol. % for $(1-x)La_2W_3O_{12}-x\,SiO_2$ to 30 mol. % for $(1-x)Nd_2W_3O_{12}-x\,SiO_2$. The maximum composite effect (increase in composite conductivity compared to the matrix conductivity) takes place for the $Nd_2W_3O_{12}$-SiO_2 system: the conductivity of the $0.7Nd_2W_3O_{12}$-$0.3SiO_2$ composite is 2.3 orders of magnitude higher

than the conductivity of $Nd_2W_3O_{12}$ and equals 3.2×10^{-2} S/cm at 900°C. For the $SrWO_4$-SiO_2 system, the composite effect is also very significant: the conductivity of $0.75SrWO_4$-$0.25SiO_2$ is two orders of magnitude higher than the conductivity of $SrWO_4$. For the $CaWO_4$-SiO_2 and $La_2W_3O_{12}$-SiO_2 systems, the composite effect is weaker: the maximum increase in composite conductivity compared to tungstate by 1 and 0.7 orders of magnitude occurs for compositions $0.94CaWO_4$-$0.06SiO_2$ and $0.97La_2W_3O_{12}$-$0.03SiO_2$ respectively.

In the four studied systems $(1-x)MWO_4 - x\ SiO_2$ (M = Ca, Sr) and $(1-x)Ln_2W_3O_{12} - x\ SiO_2$ (Ln = La, Nd), a composite conductivity effect was observed: with heterogeneous doping of corresponding tungstates with nanodispersed silicon oxide, the electrical conductivity increases by 0.7–2.3 orders of magnitude. With a sequential increase in silicon oxide content in the composite, the conductivity first increases and then, after reaching a maximum value at the maximum area of highly conductive matrix-dispersoid interfacial boundaries ($MeWO_4|SiO_2$ or $Ln_2W_3O_{12}|SiO_2$), decreases, which is due to the reduction in the area of tungstate-silica interfacial boundaries along which electron transfer occurs in composites [25 – 27], and an increase in the area of interfacial boundaries between SiO_2 dielectric grains.

For the studied systems, no connection between the composite effect and the matrix structure was revealed. Alkaline earth metal tungstates $CaWO_4$ and $SrWO_4$ have a scheelite structure (tetragonal system) [17, 23], formed by $[WO_4]]$ tetrahedra and $[MO_8]]$ dodecahedra. The conductivity values of these isostructural tungstates are quite close: at 900°C $\sigma(CaWO_4) = 5 \times 10^{-5}$ S/cm, $\sigma(SrWO_4) = 2 \times 10^{-5}$ S/cm [24]. However, in the $SrWO_4$–SiO_2 system, the maximum conductivity increase compared to the tungstate is 2 orders of magnitude, while in the $CaWO_4$–SiO_2 system it is only 1 order of magnitude (Fig. 7). Thus, in the $SrWO_4$–SiO_2 system, the composite conductivity effect is significantly stronger.

Similar results were obtained for composites based on rare earth metal tungstates. $Nd_2W_3O_{12}$ and $La_2W_3O_{12}$ have a "defective scheelite" structure with monoclinic

symmetry (space group *From* 2/ *with* [19]). This structure is based on tetrahedra [WO_4], is derived from scheelite ($CaWO_4$) and is formed by replacing three calcium atoms with two atoms of a trivalent metal [21, 23]. Despite the similar structure of the composite matrix, in the $Nd_2W_3O_{12}$–SiO_2 system, an increase in conductivity was observed during heterogeneous doping of REE tungstate with silica by 2.3 orders of magnitude, while in the $La_2W_3O_{12}$–SiO_2 system – by only 0.7 orders of magnitude.

Analysis of the morphology of the investigated composites also did not reveal significant differences: in all cases, the composite was formed by large tungstate grains (2–20 μm) and small silica grains (<1 μm). In all composites, absorption of small silica grains by large tungstate grains was observed, due to the difference in interfacial energies of MWO_4 ($Ln_2W_3O_{12}$) and SiO_2.

What is the reason for the higher composite effect in the $SrWO_4$–SiO_2 and $Nd_2W_3O_{12}$–SiO_2 systems compared to $CaWO_4$–SiO_2 and $La_2W_3O_{12}$–SiO_2? Comparison of the effective density of composites $(1-x)MWO_4-x\,SiO_2$ (M = Ca, Sr) and $(1-x)Ln_2W_3O_{12}-x\,SiO_2$ (Ln = La, Nd) showed that there is a clear correlation between the magnitude of the composite effect in the studied systems and the effective density of the composite briquettes (Table 4).

The maximum composite effect was found for the densest composites $(1-x)Nd_2W_3O_{12}-x\,SiO_2$ with an effective density of 94%, and the smallest composite effect was recorded for the loosest composites $(1-x)CaWO_4-x\,SiO_2$ with an effective density of 70%. Thus, high ceramic density is a necessary condition for the realization of the composite effect. This is not surprising, as high conductivity of composites requires the presence of a continuous highly conductive interface between the matrix and dispersed additive, which is facilitated by high ceramic density.

It should be noted that the effective density of the studied composites $(1-x)MWO_4-x\,SiO_2$ (M = Ca, Sr) and $(1-x)Ln_2W_3O_{12}-x\,SiO_2$ (Ln = La, Nd) differed significantly despite similar conditions of their briquetting and sintering. The attempt to obtain denser composites $(1-x)CaWO_4-x\,SiO_2$ and $(1-x)La_2W_3O_{12}-x\,SiO_2$ with

an effective density close to 90% (as in (1- x)$SrWO_4$- x $SiO_2$and (1- x)$Nd_2W_3O_{12}$- x SiO_2), was unsuccessful, as increasing the temperature above 1000°C led to ceramic recrystallization, and in the case of $Ln_2W_3O_{12}$- also to partial melting.

CONCLUSION

Composite solid electrolytes (1- x)MWO_4- x SiO_2(M = Ca, Sr), (1- x)$Ln_2W_3O_{12}$- x SiO_2(Ln = La, Nd) were synthesized and their thermal, structural, and electrical transport properties were investigated. Measurement of the sum of ionic transport numbers by EMF method and investigation of the pressure dependence of electrical conductivity of composites showed that they possess predominantly ionic conductivity. For all studied systems, a composite conductivity effect was discovered - an increase in electrical conductivity upon addition of nanodispersed silicon oxide to metal tungstate. The conductivity maximum is observed at silica content from 0.03 mol. fr. in composite (1- x)$La_2W_3O_{12}$- x $SiO_2$to 0.3 mol. fr. in composite (1- x)$Nd_2W_3O_{12}$- x SiO_2. The largest composite effect - an increase in electrical conductivity by 2.3 orders of magnitude - was recorded for the $Nd_2W_3O_{12}$-SiO_2system, in which the maximum conductivity value (3.2×10^{-2} S/cm at 900°C) has the composite $0.70Nd_2W_3O_{12}$-$0.30SiO_2$. It was established that the composite effect in the studied systems does not depend on the crystal structure of the composite matrix but increases with the growth of effective density of composite ceramics, which is due to the increase in the area of interfacial boundaries $MWO_4|SiO_2$(or $Ln_2W_3O_{12}|SiO_2$)), along which electrical transfer in composites is realized.

ACKNOWLEDGMENT

The research results were obtained within the framework of the state assignment of the Ministry of Science and Higher Education of the Russian Federation (project No.

123031300049-8) using the equipment of the UCCU "Modern Nanotechnologies" UrFU (reg. No. 2968), supported by the Ministry of Science and Higher Education of the Russian Federation (project No. 075-15-2021-677).

CONFLICT OF INTEREST

The authors declare that they have no conflict of interest.

REFERENCES

1. *Phipps J.B., Whitmore D.H.* // Solid State Ionics. 1983. V. 9/10. P. 123. https://doi.org/10.1016/0167-2738(83)90220-5

2. *Mateyshina Y., Slobodyuk A., Kavun V., Uvarov N.* // Solid State Ionics. 2018. V. 324. P. 196.
https://doi.org/10.1016/j.ssi.2018.04.026

3. *Ponomareva V.G., Shutova E.S.* // Solid State Ionics. 2005. V. 176. № 39/40. P. 2905.
https://doi.org/10.1016/j.ssi.2005.09.021

4. *Shigeoka H., Otomo J., Wen C.-J. et al.* // J. Electrochem. Soc. 2004. 151. P. J76.
https://doi.org/10.1149/1.1793192

5. *Tadanaga K., Imai K., Tatsumisago M., Minami T.* // J. Electrochem. Soc. 2002. V. 149. P. A773.
https://doi.org/10.1149/1.1475687

6. *Ponomareva V.G., Burgina E.B., Tarnopolsky V.A., Yaroslavtsev A.B.* // Mendeleev Commun. 2002. № 6. P. 2238. https://doi.org/10.1070/MC2002v012n06ABEH001667

7. *Guohua Jia, Chaoyang Tu, Jianfu Li et al.* // J. Alloys Compd. 2007. V. 436. P. 341. https://doi.org/10.1016/j.jallcom.2006.07.037

8. *Yiguo Su, Liping Li, Guangshe Li* // Chem. Mater. 2008. V. 20. P. 6060. https://doi.org/10.1021/cm8014435

9. *Zhiyao Hou, Chunxia Li, Jun Yang et al.* // J. Mater. Chem. 2009. V. 19. P. 2737. https://doi.org/10.1039/B818810F

10. *Jinsheng Liao, Bao Qiu, Herui Wen et al.* // Mater. Res. Bull. 2009. V. 44. P. 1863.
https://doi.org/10.1016/j.materresbull.2009.05.013

11. *Pang M.L., Lin J., Yu. M.* // J. Solid State Chem. 2004. V. 177. P. 2237. https://doi.org/10.1016/j.jssc.2004.02.031

12. *Dong Wang, Piaoping Yang, Ziyong Cheng et al.* // J. Colloid Interface Sci. 2012. V. 365. P. 320. https://doi.org/10.1016/j.jcis.2011.09.008

13. *Peiqing Cai, Cuili Chen, Qin Lin et al.* // J. Korean Phys. Soc. 2016. V. 68. №. 3. P. 443.
https://doi.org/10.3938/jkps.68.443

14. *Ulyankina A.A., Tsarenko A.D., Molodtsova T.A. et al.* // Electrochemistry. 2023. V. 59. No. 12. P. 790. https://doi.org/10.31857/S0424857023120149

15. *Pestereva N., Guseva A., Vyatkin I., Lopatin D.* // Solid State Ionics. 2017. V. 301. P. 72.
https://doi.org/10.1016/j.ssi.2017.01.009

16. *Pestereva N.N., Zhukova A.Yu., Neiman A.Ya.* // Russ. J. Electrochem. 2007. V. 43. P. 1305.

17. *Grigorieva L.F.* State Diagrams of Refractory Oxide Systems: Handbook. Issue 5. Binary Systems. Part 4. Leningrad: Nauka, 1988. 348 p.

18. *Rode E.Y., Balagina G.M., Ivanova M.M., Karpov V.N.* // Russ. J. Inorg. Chem. 1968. V. 13. P. 762.

19. *Guseva A.F., Pestereva N.N., Otcheskikh D.D., Vostrotina E.L.* // Russ. J. Electrochem. 2019. V. 55. P. 544. https://doi.org/10.1134/S1023193519060090

20. *Imanaka N., Tamura S.* // Bull. Chem. Soc. Jpn. 2011. V. 84. P. 353. https://doi.org/10.1246/bcsj.20100178

21. *Evdokimov A.A., Efremov V.A., Trunov V.K. et al.* Compounds of Rare Earth Elements. Molybdates, Tungstates. Moscow: Nauka, 1991. P. 51.

22. *Guseva A.F., Pestereva N.N.* // Russ. J. Inorg. Chem. 2023. V. 68. No. 3. P. 426.

23. *Porai-Koshits M.A., Atovmyan L.O.* Crystal Chemistry and Stereochemistry of Molybdenum Coordination Compounds USSR Academy of Sciences. Institute of Chemical Physics. Moscow: Nauka, 1974. 231 p. https://doi.org/10.31857/S0044457X2260164X

24. *Neiman A.Ya., Pestereva N.N., Sharafutdinov A.R. et al.* // Russ. J. Electrochem. 2005. V. 41. P. 598.

25. *Uvarov N.F.* Composite solid electrolytes (in Russian), Novosibirsk: ISSC SB RAS Publ. 2008. 259 p.

26. *Ulikhin A.S., Novozhilov D.V., Khusnutdinov V.R. et al.* // Electrochemistry. 2022. V. 58. No. 7. P. 380. https://doi.org/10.31857/S0424857022070143

27. *Alekseev D.V., Mateishina Yu.G., Uvarov N.F.* // Electrochemistry. 2022. V. 58. No. 7. P. 394. https://doi.org/10.31857/S0424857022070039

Table 1. Solid-phase synthesis mode of tungstates MWO_4 (M = Ca, Sr) and $Ln_2W_3O_{12}$ (Ln = La, Nd)

Stage	MWO_4 (M = Ca, Sr)		$La_2W_3O_{12}$		$Nd_2W_3O_{12}$	
	t , °C	τ, h	*t* , °C	τ, h	*t* , °C	τ, h
1	700	10	700	10	700	25
2	800	15	800	15	800	55
3	900	24	900	24	900	85
4	1000	30	1000	30	1050	85

Table 2. Ratio of molar fraction (mol. fr.) and volume fraction (vol. fr.) of SiO_2 in composites

$CaWO_4$-SiO_2		$SrWO_4$-SiO_2		$La_2W_3O_{12}$-SiO_2		$Nd_2W_3O_{12}$-SiO_2	
mol. fr. SiO_2	vol. fr. SiO_2	mol. fr. SiO_2	vol. fr. SiO_2	mol. fr. SiO_2	vol. fr. SiO_2	mol. fr. SiO_2	vol. fr. SiO_2
0	0	0	0	0	0	0	0
0.05	0.025	0.01	0.004	0.01	0.002	0.03	0.005
0.06	0.030	0.03	0.011	0.03	0.005	0.10	0.016
0.10	0.050	0.05	0.018	0.05	0.008	0.15	0.025
0.15	0.080	0.10	0.038	0.20	0.035	0.25	0.046
0.30	0.200	0.15	0.059	0.30	0.060	0.30	0.060
0.50	0.320	0.17	0.068	1	1	0.40	0.088
0.80	0.660	0.25	0.106			0.50	0.127
1	1	0.30	0.133				
		0.60	0.350				
		0.70	0.454				
		1	1				

Table 3. Average effective density of composites $(1-x)MWO_4 - x\ SiO_2$ and $(1-x)Ln_2W_3O_{12} - x\ SiO_2$

	$(1-x)CaWO_4 - x\ SiO_2$	$(1-x)SrWO_4 - x\ SiO_2$	$(1-x)La_2W_3O_{12} - x\ SiO_2$	$(1-x)Nd_2W_3O_{12} - x\ SiO_2$
Effective density, %	70	88	78	94

Table 4. Comparison of average effective density of composite briquettes $(1-x)MWO_4 - x\ SiO_2$ (M = Ca, Sr) and $(1-x)Ln_2W_3O_{12} - x\ SiO_2$ (Ln = La, Nd) with composite effect value

Parameter	$(1-x)CaWO_4 - x\ SiO_2$	$(1-x)La_2W_3O_{12} - x\ SiO_2$	$(1-x)SrWO_4 - x\ SiO_2$	$(1-x)Nd_2W_3O_{12} - x\ SiO_2$

Effective density, %	70	78	88	94
Composite effect (order)	0.7	1	2	2.3

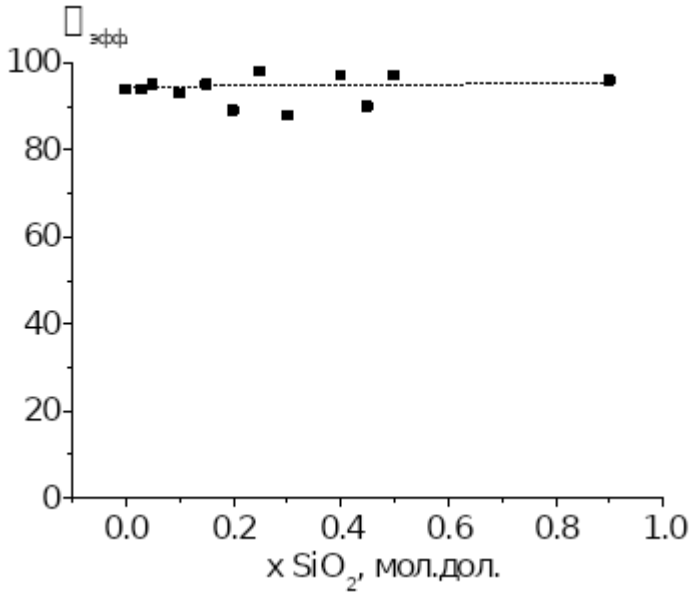

Fig. 1. Concentration dependence of effective density of composites $(1-x)Nd_2W_3O_{12}-xSiO_2$.

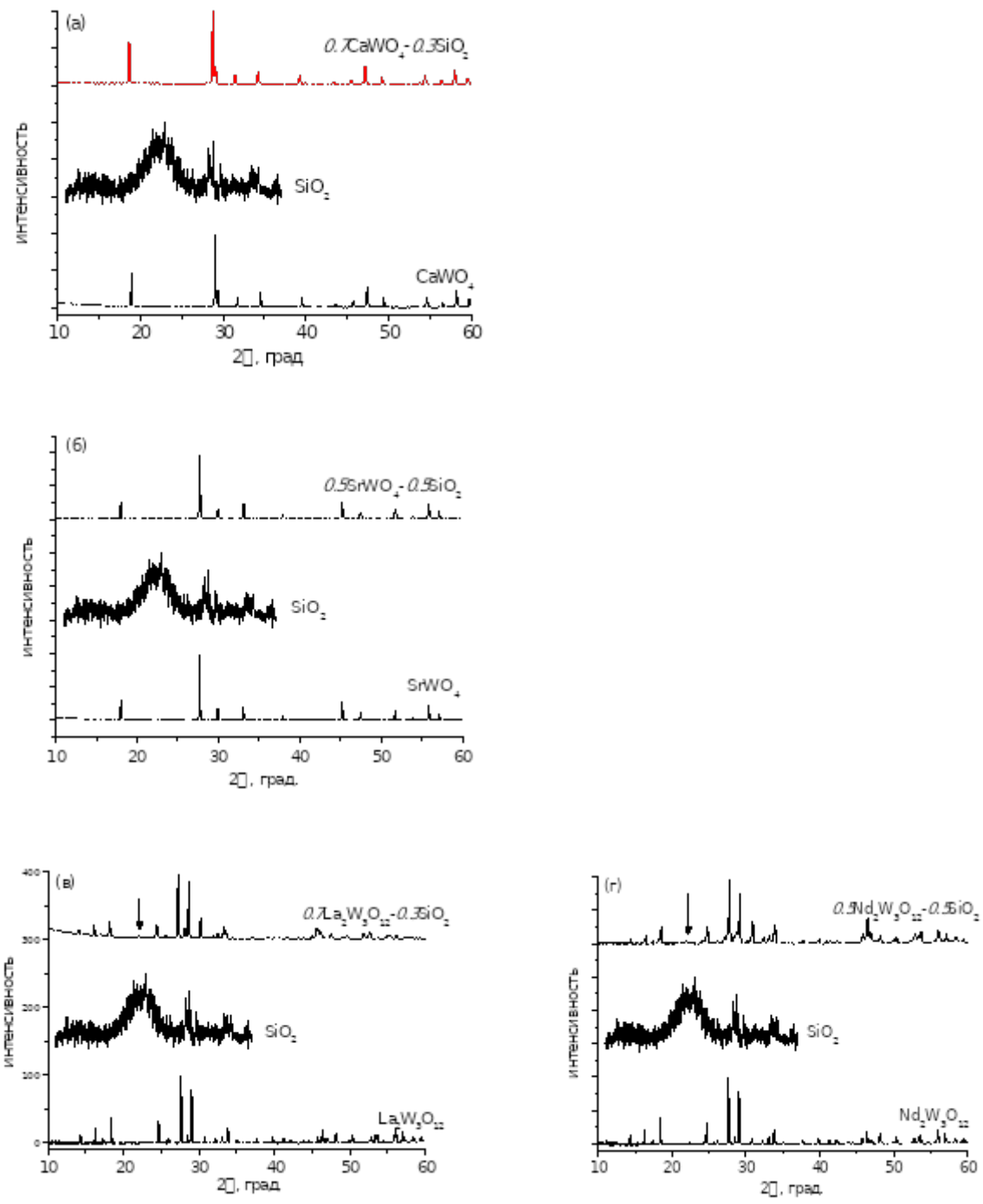

Fig. 2. XRD data of composites (1- *x*)MWO_4- *x* SiO_2(M = Ca (a), Sr (b)) and (1- *x*)$Ln_2W_3O_{12}$- *x* SiO_2(Ln = La (c), Nd (d)).

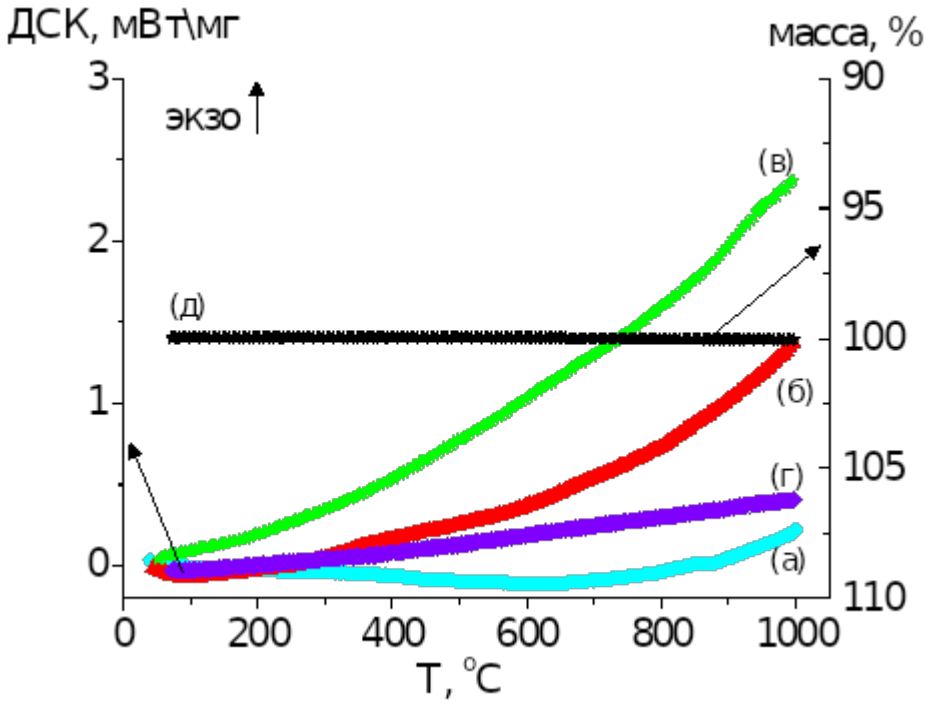

Fig. 3. TG-DSC results of mixtures 0.5CaWO $_4$-0.5SiO $_2$(a), 0.5SrWO $_4$-0.5SiO $_2$ (b), 0.5Ln $_2$W $_3$O $_{12}$-0.5SiO $_2$(c) and 0.5Nd $_2$W $_3$O $_{12}$-0.5SiO $_2$(d), mass of composite 0.5CaWO $_4$-0.5SiO $_2$(e).

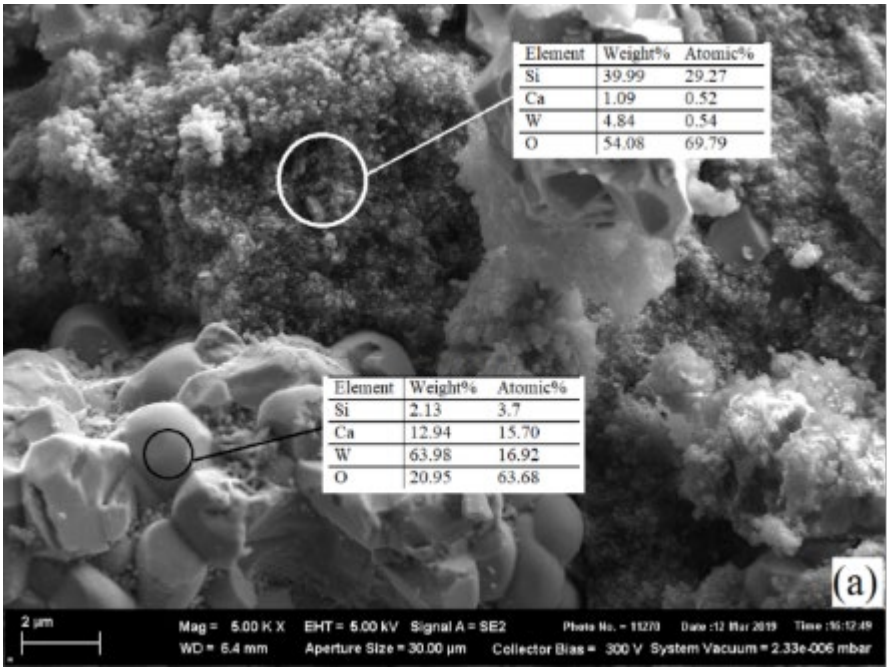
Element Weight% Atomic%
Si 39.99 29.27
Ca 1.09 0.52
W 4.84 0.54
O 54.08 69.79
Element Weight% Atomic%
Si 2.13 3.7
Ca 12.94 15.70
W 63.98 16.92
O 20.95 63.68
(а)
2 µm
Mag = 5.00 K X EHT = 5.00 kV Signal A = SE2
WD = 6.4 mm Aperture Size = 30.00 µm Collector Bias = 300 V System Vacuum = 2.33e-006 mbar

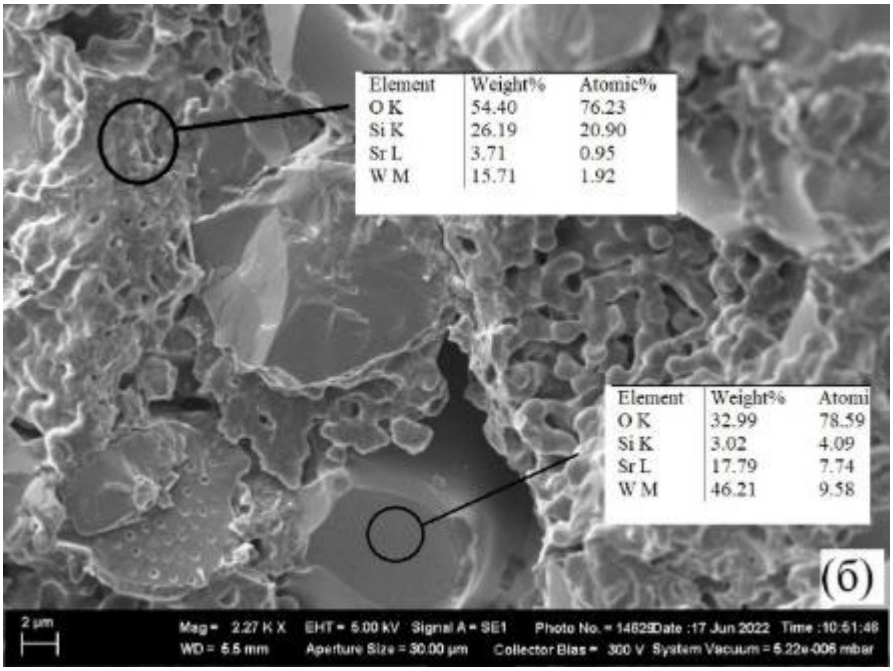
Element Weight% Atomic%
O K 54.40 76.23
Si K 26.19 20.90
Sr L 3.71 0.95
W M 15.71 1.92
Element Weight% Atomi
O K 32.99 78.59
Si K 3.02 4.09
Sr L 17.79 7.74
W M 46.21 9.58
(б)
2 µm
Mag = 2.27 K X EHT = 5.00 kV Signal A = SE1 Photo No. = 14629 Date :17 Jun 2022 Time :10:51:46
WD = 6.5 mm Aperture Size = 30.00 µm Collector Bias = 300 V System Vacuum = 6.22e-006 mbar

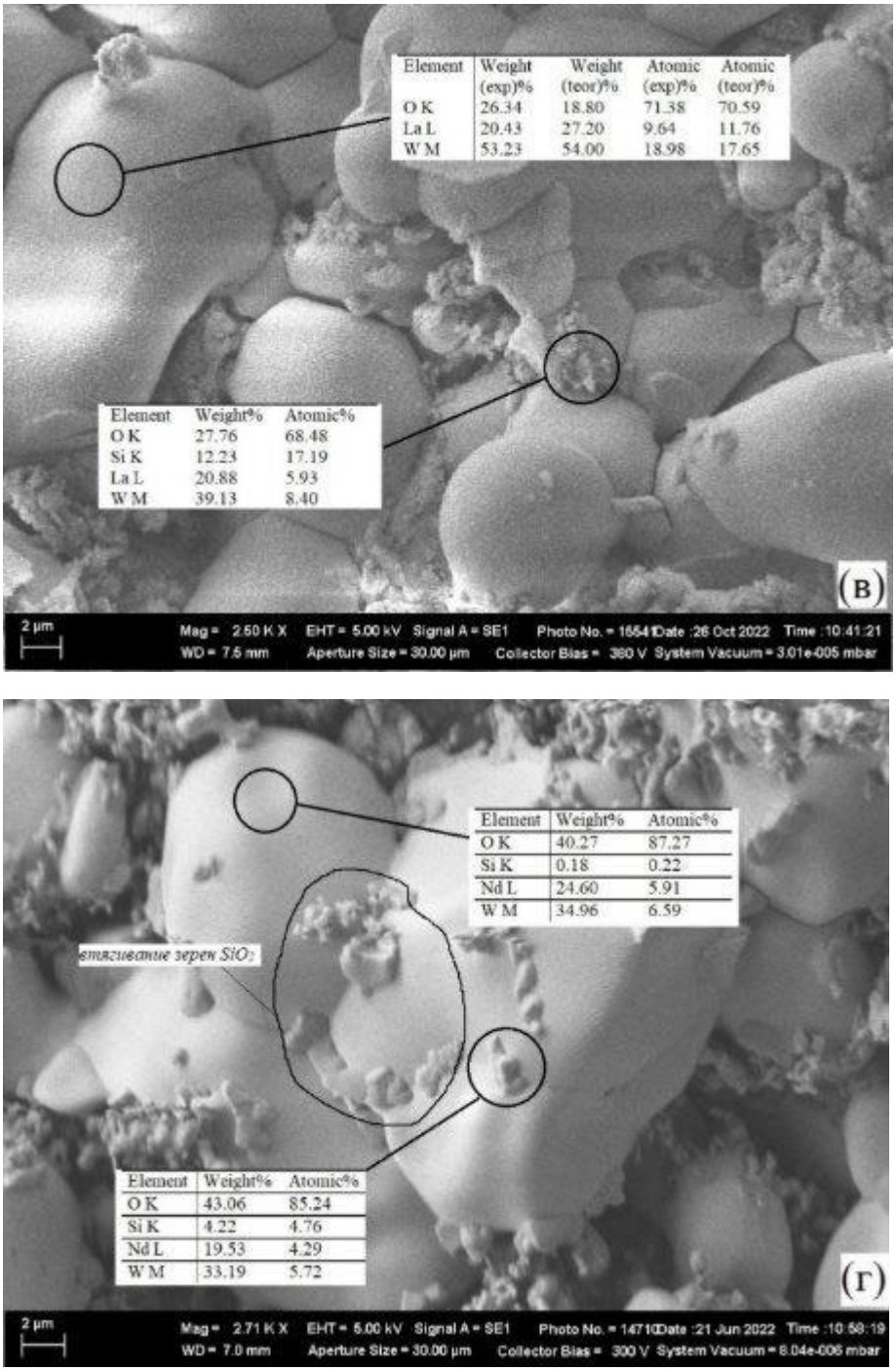

Fig. 4. SEM images and elemental composition of composites according to EDS data: 0.7$CaWO_4$–0.3SiO_2(a), 0.75$SrWO_4$–0.25SiO_2(b), 0.7$La_2W_3O_{12}$–0.3SiO_2(c), 0.7$Nd_2W_3O_{12}$–0.3SiO_2(d).

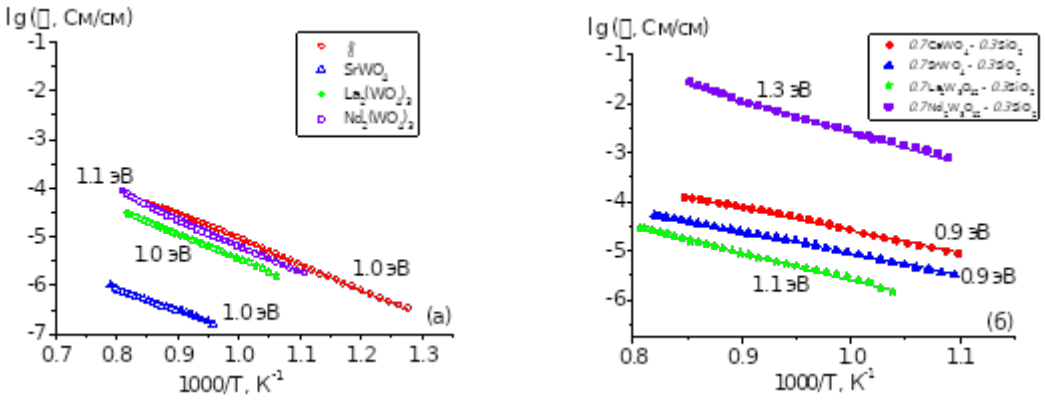

Fig. 5. Temperature dependence of electrical conductivity of pure tungstates (a) and composites 0.7MWO_4–0.3SiO_2 (M = Ca, Sr), 0.7$Ln_2W_3O_{12}$–0.3SiO_2 (Ln = La, Nd) (b) on inverse temperature.

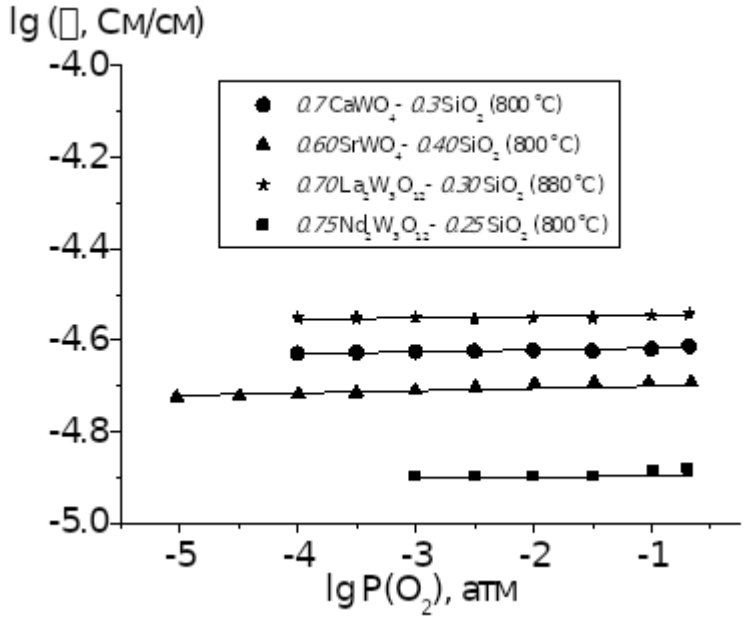

Fig. 6. Dependence of electrical conductivity of composites $(1-x)MWO_4 - x\ SiO_2$ and $(1-x)Ln_2W_3O_{12} - x\ SiO_2$ on oxygen partial pressure in the gas phase.

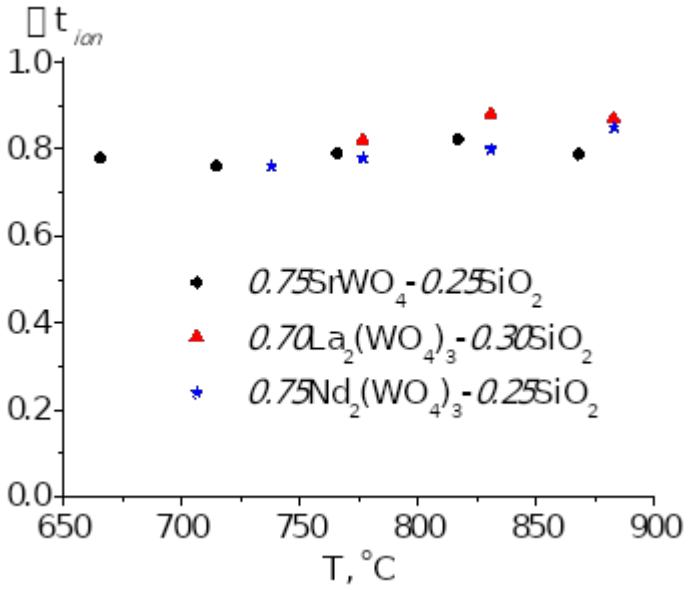

Fig. 7. Temperature dependence of the sum of ionic transport numbers for composites 0.75SrWO $_4$–0.25SiO $_2$, 0.70La $_2$W $_3$O $_{12}$–0.30SiO $_2$ and 0.75Nd $_2$W $_3$O $_{12}$–0.25SiO $_2$.

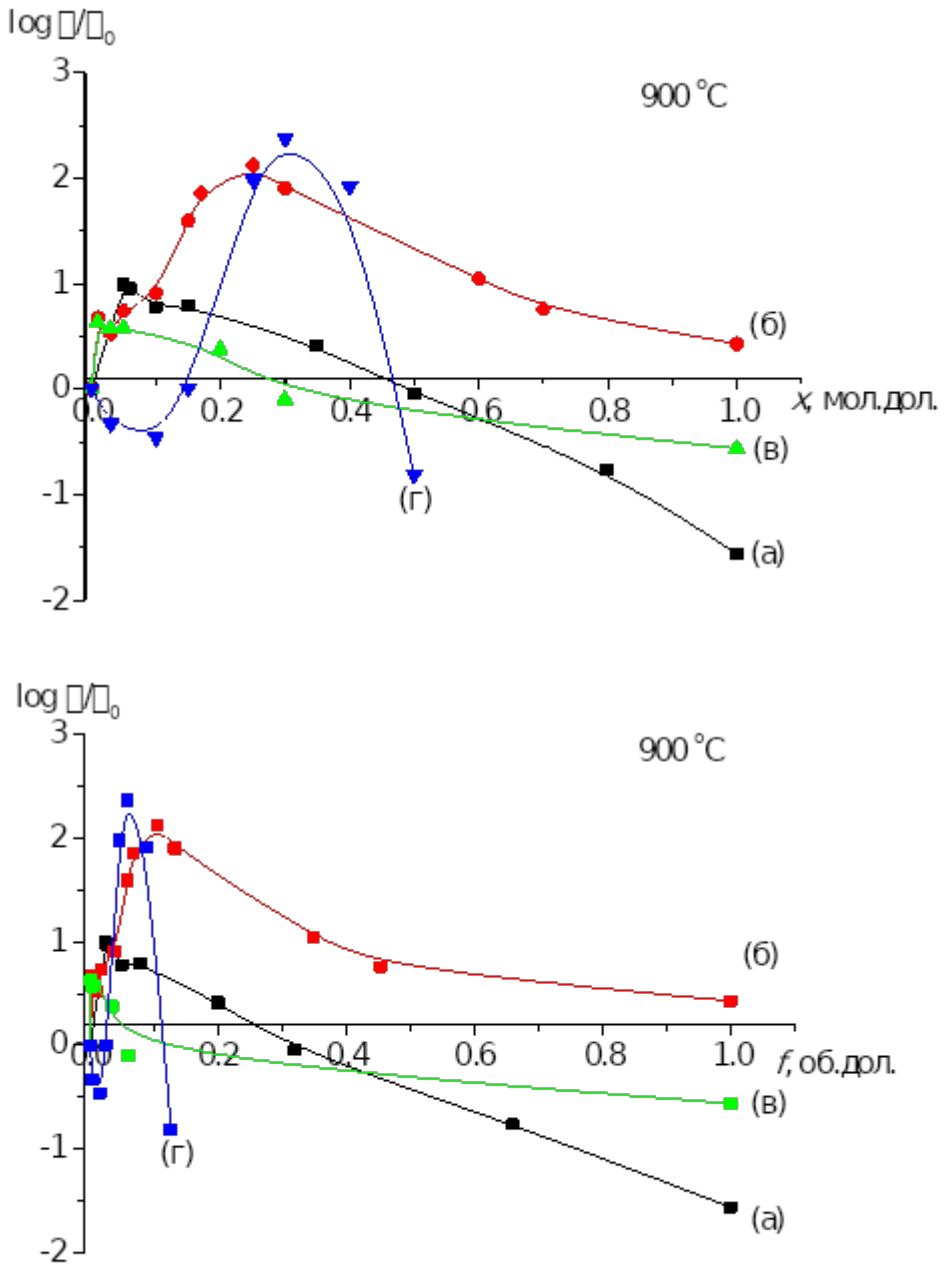

Fig. 8. Dependence of relative electrical conductivity of composites $(1-x)CaWO_4 - x\,SiO_2$(a), $(1-x)SrWO_4 - x\,SiO_2$(b), $(1-x)La_2W_3O_{12} - x\,SiO_2$(c) and $(1-x)Nd_2W_3O_{12} - x\,SiO_2$(d) on molar and volume fraction of SiO_2 at 900°C.